Electrocatalysis (2014) 5:279–287
DOI 10.1007/s12678-014-0194-1

Obtaining Clean and Well-dispersed Pt NPs with a Microwave-assisted Method

V. Armendáriz · C. A. Martins · H. E. Troiani · L. C. S. de Oliveira · J. M. Stropa · G. A. Camara · M. E. Martins · P. S. Fernández

Published online: 20 March 2014

Abstract Carbon-supported platinum nanoparticles Pt/C (NPs) are used in many fields of science. These kinds of materials have been extensively studied in electrochemistry due to the fact that they are applied in fuel cell technology. Although there are a myriad of methods for Pt NP synthesis, the need for obtaining Pt/C NPs with a good dispersion (covering over the entire support), a narrow size distribution, and clean surface (among other parameters) is far to be overcome. On this sense herein we describe a very easy and quick method of synthesis of highly dispersed Pt NPs followed by a simple electrochemical cleaning step. The catalysts were electrochemically characterized by studying their behavior in 0.5 M H_2SO_4 and also by using CO as a probe during the CO electro-oxidation reaction (COEOR). This paper shows how to obtain highly dispersed and clean Pt/C NPs that produce very reproducible results. Besides, we demonstrate how the presence of impurities negatively affects the electrochemical reproducibility of Pt NPs with a clear impact on their catalytic activity.

V. Armendáriz · M. E. Martins · P. S. Fernández (✉)
INIFTA, Universidad Nacional de La Plata,
Diagonal 113 y Calle 64, La Plata, Buenos Aires, Agentina
e-mail: pablosf23@yahoo.com.ar

C. A. Martins · L. C. S. de Oliveira · J. M. Stropa ·
G. A. Camara (✉)
Institute of Chemistry, UFMS, 549 Av. Filinto Muller 1555,
79070-900 Campo Grande, MS, Brasil
e-mail: giuseppe.silva@ufms.br

H. E. Troiani
Centro Atómico Bariloche (CNEA), CONICET, Instituto Balseiro,
CP 8400, S.C. de Bariloche, Río Negro, Argentina

J. M. Stropa
Universidade Estadual de Mato Grosso do Sul, Unidade de Naviraí,
Emílio Mascoli, 275, 79950-000 Naviraí, MS, Brasil

Keywords Platinum nanoparticles · Microwave-assisted synthesis · Cleaning process · Agglomeration of nanoparticles · Active surface area · CO probe

Introduction

There are a lot of methods to synthesize Pt/C NPs [1–5]. Most of them consist in dispersing the desired quantities of carbon, Pt salts, and water. The most common way of obtaining this kind of catalyst is the polyol method, in which the aqueous solution contains a polyalcohol (most commonly ethylene glycol) [6]. The NPs are obtained after boiling the dispersion for a few hours, because during this process, the alcohol acts as reducing agent and as surfactant at the same time [6]. Despite its simplicity, it is necessary to add some other surfactant if metallic NPs with narrow size distribution are required. On the other hand, the use of surfactants commonly renders materials with important amounts of impurities, which means that if they are not used with proper care, the results obtained with these catalysts have very poor reproducibility.

In the last years, researchers of Poitiers [7], Alicante [8], and Leiden [9] have overcome the problem of cleaning Pt NPs. These groups demonstrate that the voltammetric response in sulfuric acid shows very well-developed adsorption-desorption hydrogen-sulfate peaks [7–9]. In [7] and [8], the authors obtained extremely clean Pt NPs by using sodium polyacrylate (PA) as a surfactant and a careful centrifugation process, which allow cleaning and separating NPs with slightly the same size and shape. In [9], the authors prepared the NPs through two methods, in one case the same method used in [7] and [8] was utilized, and in the second approach a similar process was used but changing PA

by polyvinylpyrrolidone (PVP). They cleaned the NPs very efficiently by using a mixture of H_2O_2 and H_2SO_4. However, in these three cases the Pt NPs are not supported, being deposited on a flat gold electrode before performing the electrochemical experiments.

In order to obtain results more closely related to the fuel cells research field, it is crucial to perform experiments with well-dispersed, narrow size distribution, and clean carbon-supported Pt NPs. There are a lot of papers connected with this topic in the literature, but, unfortunately the success in obtaining Pt/C NPs with those characteristics is quite poor. Other undesired fact is that the literature is plenty of papers where the electrocatalytic behavior of NPs is analyzed, but these materials are not properly clean. Also, most of these works do not show (or even discuss) the uncertainty in the analysis. In a previous work, we investigate how the electro-oxidation of glycerol is affected by the degree of cleaning of Pt NPs [10] and mention that different traditional cleaning procedures as that mentioned in [7–9] and washing with several solvents as water, acetone, ethanol, etc. are not able to efficiently clean the NPs anchored on a carbon support. In this sense, here we delve into the question of the influence of NP cleaning degree in its electrochemical response, by using CO as a probe molecule. Moreover, we obtained NPs with a high degree of dispersion over the support and improved the control over the cleaning process.

Taking into account the very interesting results obtained by using PA we decided to use this surfactant in the polyol method, which allows obtaining NPs with excellent dispersion over the carbon support and with a narrow size distribution NPs. Besides, using a regular microwave to assist the synthesis, the time was reduced from some hours (typically 1–3 h) to 90 s [11–13].

Experimental

Synthesis of Pt NPs

Pt NPs/C were synthesized by using the polyol method. In this case, we used the protocol followed in a previous work [14] but with some modifications. Briefly, we mixed 8.8 mL of $1.74.10^{-2}$ M of H_2PtCl_6, 120 mg of Carbon Vulcan XC72® (20 % Pt), and 38 mL of solution 3:1 of ethylene glycol (EG)/water. In this protocol, we replaced the polyvinylpyrrolidone (PVP, commonly used during the synthesis of Pt NPs) by sodium polyacrylate (PA). The vessel containing the mixture was heated during 90 s using a household microwave oven, as described in [11]. Three different syntheses were performed by varying the PA/Pt ratio (the ratio was adjusted to 0, 0.5, and 5).

Preparation and Characterization of the Electrodes

Electrochemical experiments were carried out employing a three-electrode cell in aqueous acid medium. Carbon-supported NPs were used as a working electrode, while a high area Pt electrode was used as counter electrode (CE), and the potentials were measured against a reversible hydrogen reference electrode (RHE) in the same electrolyte and are presented in the same scale. The working electrode was prepared as follows: a polycrystalline gold disk of 0.5 cm^2 of geometric area used as support was first polished to a mirror finish and rinsed in alkaline $KMnO_4$ solution and acid H_2O_2 solution. Afterward, the disk was thoroughly washed with Milli-Q® water and heated on a plate at 50±2 °C. Meanwhile, 1 mg of the Pt/C powder was dispersed in 2-propanol and 50-μL Nafion® 5 % by ultrasonic bath for 30 min in order to obtain a highly homogeneous dispersion. Then, an aliquot of 25 μL from the dispersion and 50 μL of diluted Nafion® solution (1 mL of Nafion® 5 %:20 mL of 2-propanol) was applied over the disk. Before each experiment, the electrode was washed with water with the aim of pulling out some particles not well adhered. All electrochemical runs were performed at 25 °C. An aqueous solution containing 0.5 M H_2SO_4 under oxygen-free conditions was used to perform the electrochemical cleaning, to characterize the electrode surface, and to test the electrochemical activity of Pt NPs toward CO electro-oxidation reaction (COEOR).

TGA curves were obtained in a TGA Q50 (TA Instruments-Waters, LLC) equipment. N_2 was used as balance with a purge rate of 40 mL min^{-1}. The sample gas was an oxidant atmosphere (synthetic air), with a purge rate of 60 mL min^{-1}. The heating rates were of 10 °C min^{-1}. Masses of all samples were around 3 mg. Platinum pans were used for all measurements.

X-ray diffraction patterns (XRD) of the samples were recorded in a Bruker D8 powder diffractometer equipped with a monochromatic CuKα X-ray source and an internal standard for silicon powder. The diffractometer is also equipped with a göbel mirror in the incident beam and a parallel-slit analyzer in the diffracted beam. Diffraction data were collected by step scanning with a step size of 0.02° 2θ in the range 5–90°, with a scan step of 2 s.

TEM and HR-TEM experiments were performed in a CM 200 Philips transmission electron microscope before and after the electrochemical treatment of the catalyst. The microscope operates with a LaB6 emission gun. TEM is equipped with an ultratwin objective lens, and it was operated at 200 keV.

Results and Discussion

Characterization of the Catalysts

Figure 1 shows the thermal gravimetric analysis (TGA) for the Pt/C catalysts with PA/Pt ratios of 0, 0.5, and 5.0. The weight loss curves show that the processes of thermal decomposition occur in 3, 4, and 3 steps, respectively. The first loss of mass happens between 262 and 272 °C (the exact temperature is dependent on the catalyst) and is probably due to the elimination of some residues of ethylene glycol and water. The second loss of mass occurs in a range of temperatures (260–460 °C) and is more intense than the first one, meaning that more than a half of the initial masses are lost. For PA/Pt=0.5 the weight loss takes place in two steps. Nearly 40 % of the mass is lost between 263 and 460 °C, followed by a second fall between 460 and 520 °C. The exact cause of this unique behavior observed for PA/Pt=0.5 is beyond the scope of this work but will be investigated in the due course. This second weight loss is attributed to the thermal decomposition of both PA [15] and Carbon VULCAN XC72® [16]. After a thin plateau, a last decrease of mass is observed at temperatures ranging 450–630 °C (again, each catalyst presents a specific temperature), probably related to the oxidative decomposition of carbonaceous residues formed in the previous step or to the oxidation of carbon atoms which interact more strongly with the metal. At the end of the heating procedure, the remaining masses are due to platinum. The final mass for PA/Pt=0.0 corresponds to 10.1 % of the initial one, suggesting that part of platinum is not reduced (or lost for processes as, e.g., dissolution) when PA is absent. For the catalysts synthesized in the presence of PA, the final masses are of 17.5 and 16.1 % of the initial mass for PA/Pt=0.5 and PA/Pt=5.0, respectively, which could mean that the metal load is lower than the nominal composition (20 %). However, the presence of important amounts of residues from the synthesis (that do not account for the mass of platinum) cannot be discarded.

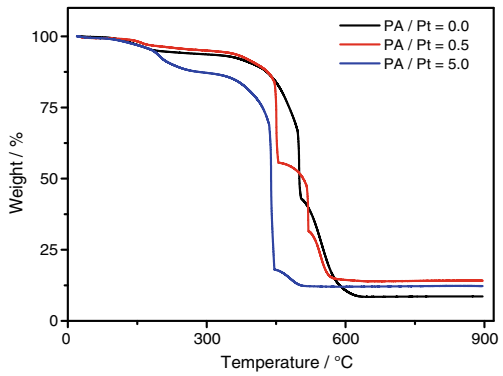

Fig. 1 TGA data of PA/Pt=0 (*black line*), 0.5 (*red line*), and 5.0 (*blue line*) in synthetic air. Heating rates were of 10 °C min^{-1}

TEM and HR-TEM micrographs of the as-prepared NPs are shown in Fig. 2. Size distribution histograms (not shown) have been drawn taking the information of several images as those shown in Fig. 2. Table 1 exhibits the Pt NPs size for all the catalysts, before and after the cycling procedure (see next section). Both, the NP size mean value and the corresponding standard errors are informed. The histograms were fitted with a log-normal distribution.

Figure 2 shows that when low amounts of PA are used (PA/Pt=0 and PA/Pt=0.5), a lot of particles agglomerate (which makes the determination of the NPs size more difficult and less representative of the sample). For instance, HR-TEM images (Fig. 2b, d, and f) exhibit NPs presenting different shapes, most of them rounded and some with truncated forms. However, when the PA/Pt ratio is increased to 5.0, the NPs synthesized are smaller and better distributed over the carbon support. Overall, results of Fig. 2 demonstrate the influence of PA as an agent for the control of the NP average size.

Figure 3 shows the X-ray diffraction pattern corresponding to the as-prepared NPs supported on carbon. The X-ray spectrum exhibits both the peak corresponding to VULCAN XC72® and those peaks corresponding to Pt nanoparticles. The peak corresponding to the (002) reflection of the carbon structure is clearly seen in the diffractogram. It confirms the presence of graphitic planes in the structure of carbon VULCAN XC72® . All the other peaks correspond to Pt NPs. Here we assume that the broadening of the peaks is mainly due to the small particles size. In consequence, from the broadening of the peak corresponding to the (111) reflection of Pt (this peak is the more intense and less affected by the measurement's noise) combined with the use of Scherrer equation it was possible to estimate the crystallite size. Results in Table 1 demonstrate that sizes determined by TEM and XRD follow a similar trend. Thus, PA seems to act lowering the NP and crystallite sizes. Besides, the fact that these values are similar confirms that these Pt NPs are mostly single crystals as also can be deduced from the HR-TEM images.

Electrochemical Characterization of the As-prepared Catalyst

The electrochemical characterization was carried out in 0.5 M H_2SO_4 and also by studying the CO electro-oxidation reaction (COEOR). In all cases, the surfaces of the fresh NPs are partially blocked, and consequently, the characteristic voltammetric features deviate from that of clean carbon-supported Pt NPs [10]. Therefore, in order to get a general view of the cleaning and degradation process of our catalyst, the NPs were submitted to 50 voltammetric cycles between 0.05 and 1.45 V in 0.5 M H_2SO_4. This procedure was

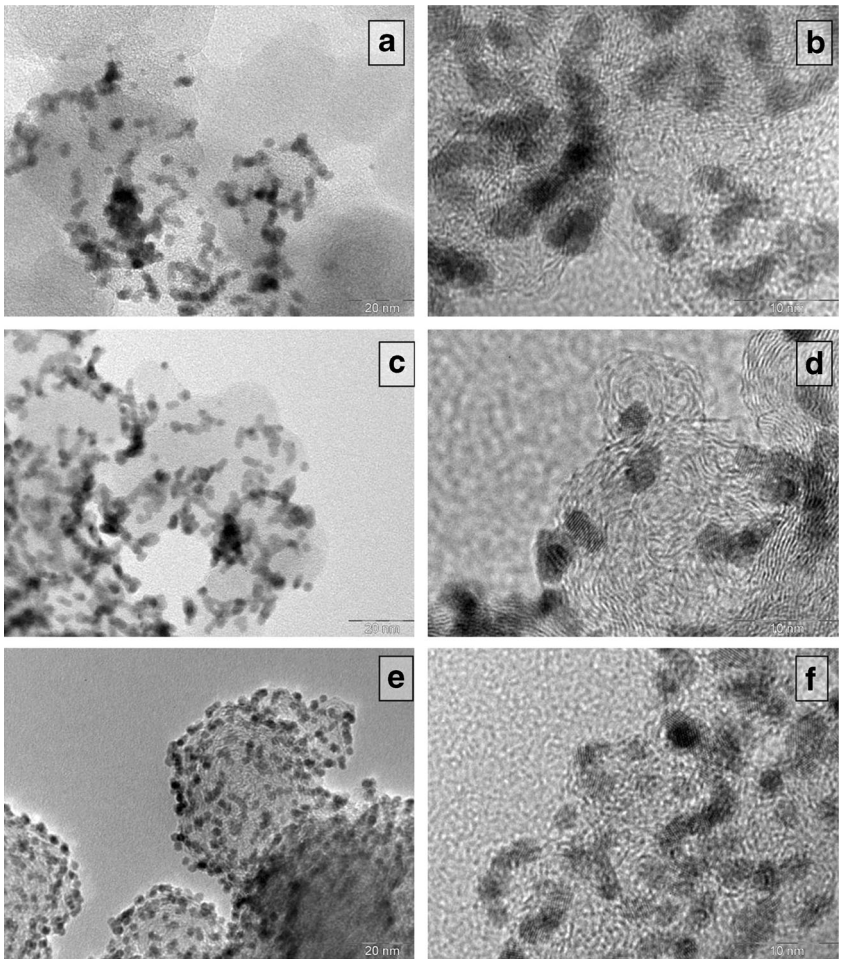

Fig. 2 TEM and HR-TEM images of PA/Pt=0 (**a**, **b**), 0.5 (**c**, **d**), and 5.0 (**e**, **f**). The NPs synthesized with lower amounts of PA (**a**–**d**) are larger than PA/Pt=5.0 (**e**, **f**). In (**e**, **f**) the particles are visually better distributed over the carbon support and present a small agglomeration degree

monitored by analyzing the features of the voltammogram of Pt in acid solution.

Figure 4 shows a progressive change of the voltammetric profile with the number of cycles for PA/Pt=5.0 (all catalysts follow a similar behavior). On this sense, cyclic voltammetry (CV) is a very useful tool to evaluate the surface state of a huge variety of materials. In the case of Pt, the fact that the response of this material (Pt bulk) in several electrolytes is well known makes the voltammetric response with number of cycles a unique in situ evaluation tool in a very simple and sensitive manner. At the beginning of the potential cycling (cycle 2, black line), a typical response of a Pt blocked surface can be seen, in which H– and O-electroadsorption and electrodesorption are hindered. Nevertheless, as the electrode

Table 1 Pt NP size distribution before (as-prepared) and after (cycled) 50 voltammetric cycles. Results obtained after DRX result fitting are shown in the last column

Sample	Fresh NPs size / nm	Cycled NPs size / nm	Crystallite size / nm
PAA/Pt=0	2.8±0.1	3.5±0.1	3.0
PAA/Pt=0.5	2.76±0.05	3.0±0.2	2.8
PAA/Pt=5	2.36±0.08	2.9±0.8	2.6

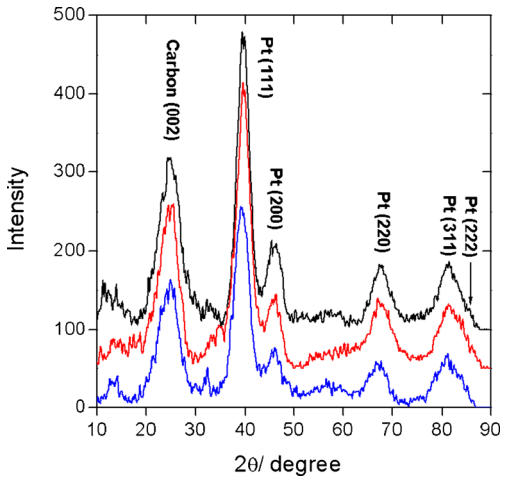

Fig. 3 X-ray diffraction spectrum for carbon-supported platinum NPs. The angles corresponding to the planes of C and Pt are specified inside the figure

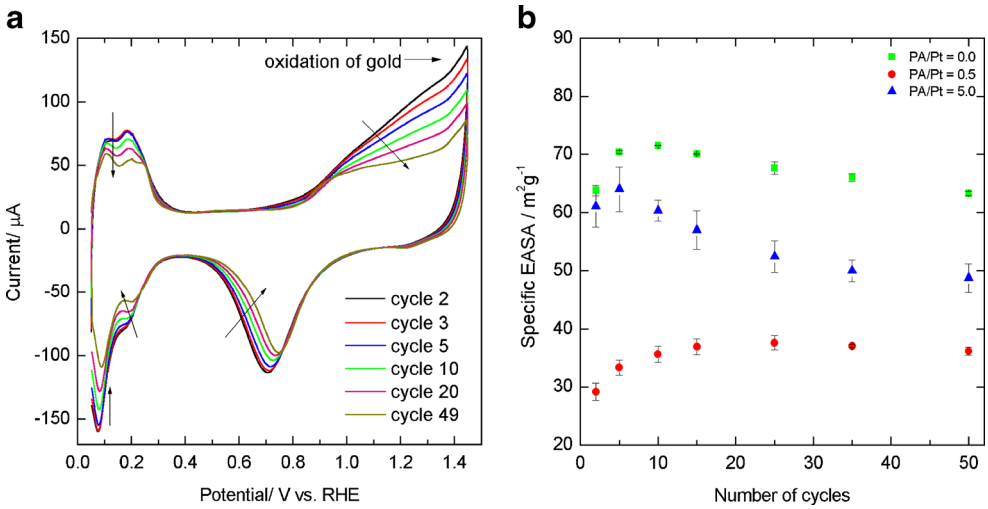

Fig. 4 **a** Cyclic voltammograms obtained during the electrochemical cleaning for cycles 2 (*black*), 3 (*red*), 5 (*blue*), 10 (*green*), 20 (*pink*), and 49 (*dark yellow*) in 0.5 M H_2SO_4. v= 0.02 V s^{-1}. **b** ECSA changes for the three catalyst as a function of the number of potential cycles

is cycled a progressive diminution of the currents is seen. Consequently, we noted a decrease in the charge corresponding to all voltammetric peaks, namely, (i) H adsorption-desorption and (ii) Pt oxide formation and Pt oxide reduction. Parallel to the cleaning process, we interpret this lowering of current in terms of a loss in the electrochemical surface area (ECSA, seen in Fig. 4b), probably caused by degradation and coarsening of Pt NPs. Besides, the formation and reduction of Pt oxides become more reversible, approaching the behavior showed by clean polycrystalline Pt.

In order to quantify the effect of cycling on each catalyst, we followed the change of relative H-electrodesorption charge (expressed as the specific area) with the number of cycles (Fig. 4b). Figure 4b shows similar behavior for the three catalysts. At the beginning of the cycling protocol, ECSA rapidly increases. Such increase is followed by the establishment of a little plateau, which is somewhat dependent on the amount of PA (an expected behavior, since different PA ratios would generate NPs with different amounts of impurities and different sizes). Afterward, the ECSA continuously diminishes up to the end of the cleaning process. As discussed in a previous work [10], such behavior can be explained in terms of different processes taking place during the voltammetric cycling. Namely, the cleaning of NPs contributes to expose more active sites to the solution and then to the increase in the ECSA. On the other hand, once clean, these sites are more exposed to processes as irreversible dissolution of Pt, Ostwald ripening, and detachment of the NPs, which contribute to the decrease of ECSA [17]. In order to follow such processes, we performed TEM and HR-TEM with the cycled NPs and confirm that this procedure generates important changes in the catalyst (Table 1 and Fig. 5). TEM measurements (Fig. 5) before and after the electrochemical cycling confirm the growing and agglomeration of nanoparticles with the cleaning procedure. The fact that NP diameter increases with cycling confirms the occurrence of ripening and/or coarsening. Besides, as expected, this effect was more prominent on the smaller NPs (PA/Pt=5). The general behavior of ECSA evidences that in the early cycles the cleaning of NPs dominates the changes in the ECSA, but subsequently, the processes which produce a decrease in the ECSA become most important. Interestingly, the specific features are different for the three catalysts. PA/Pt=5 shows an increasing of ECSA during the first cycles, indicating that the cleaning process is only determinant at the beginning of the cleaning. Due to this result and to the fact that PA/Pt=5 NPs are those which presented a

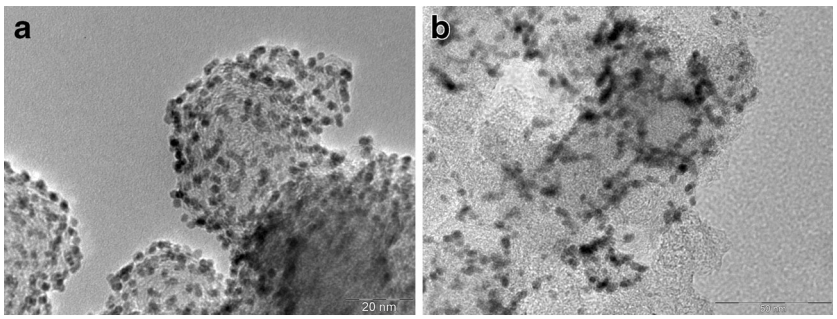

Fig. 5 TEM images of PA/Pt= 5.0, before (**a**) and after (**b**) 50 electrochemical cycles

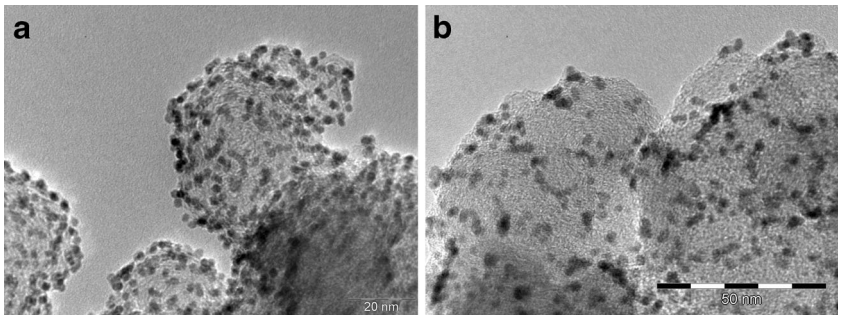

Fig. 6 HR-TEM images of PA/Pt=5.0, before (**a**) and after (**b**) 10 cleaning cycles

better dispersion onto the carbon support and more uniform sizes, we decided to repeat the electrochemical procedure only with PA/Pt=5, but limiting it to 10 cycles, as an attempt to avoid to damage the nanoparticles.

Electrochemical Characterization and Cleaning of PA/Pt=5 Catalyst

Figure 6 shows TEM images taken with fresh (Fig. 6a) and clean PA/Pt=5 NPs (Fig. 6b), while Fig. 7a shows the voltammetric behavior of the catalyst during the 10 first cleaning cycles. Here is important to note that using the voltammetric profile of electrodes containing carbon-supported Pt nanoparticles and Nafion® (which is the most common scenario in fuel cell research) as a criterion for checking the cleaning of NPs is not a trivial task, since their electrochemical response is markedly different from that of bulk Pt.

As we pointed out before and will show experimentally, the level of cleaning of this type of catalyst is crucial to obtain reproducible results. Figure 4a, b demonstrates how the voltammetric features of these materials change continuously during cycling, since Pt NPs suffer important and irreversible changes during all the cycling process, even after several cycles. This fact imposes important restrictions to the analysis because, unlike bulk Pt, here it is not possible to perform an electrochemical cycling up to obtain a reproducible voltammogram (indeed, it is possible, but the voltammograms will tend to accommodate only after very important structural changes, as agglomeration and coarsening of NPs).

Other interesting behavior (Fig. 7a) concerning this material is that the cycling strongly affects the Pt oxidation domain, while producing only minor changes in the H desorption region. Such discrepancies suggest that the poor definition of the H adsorption-desorption peaks is an intrinsic characteristic of this type of electrodes.

Taking into account that the Pt oxidation region is the most affected by the presence of impurities on the surface of NPs, we decided to use this region to monitor how the NPs evolve during the cleaning procedure. As stated before, in this region we have several processes which contribute to the total charge (Q_T) measured in the Pt oxidation domain, namely:

1. Reversible oxidation of Pt to form oxides (Q_{Pt-PtO_x}).
2. Irreversible oxidation of Pt to produce ions ($Q_{Pt-Pt^{+n}}$).
3. Oxidation of carbon (Q_{C-CO_x}).
4. Oxidation of impurities (Q_{imp}).
5. And finally, a small and constant contribution from the oxidation of Au disk can be seen between 1.40 and 1.45 V (Q_{Au-AuO_x}).

Thus, the global oxidation charge (Q_T) obtained by integration of the currents in the Pt oxidation region can be assumed to be the sum of all these contributions:

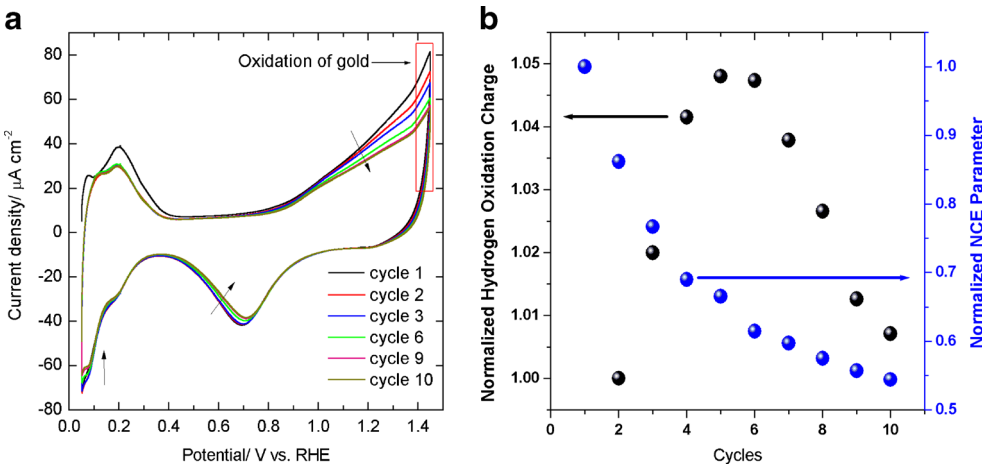

Fig. 7 **a** Cyclic voltammograms obtained during the electrochemical cleaning for cycles 1 (*black*), 2 (*red*), 3 (*blue*), 6 (*green*), 9 (*pink*), and 10 (*dark yellow*) in 0.5 M H_2SO_4. v= 0.02 V s^{-1}. **b** Normalized hydrogen oxidation charge and NCE parameter vs. the number of cleaning cycles

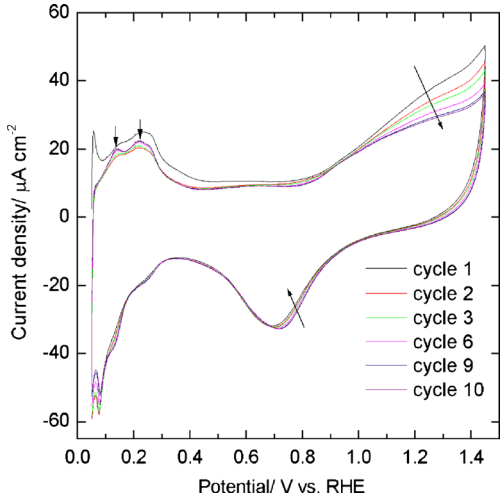

Fig. 8 Cyclic voltammograms obtained during the electrochemical cleaning of Pt/C E-TEK® (20 wt%) in 0.5 M H_2SO_4. v=0.02 V s^{-1}

$$Q_T = Q_{Pt-PtO_x} + Q_{Pt-Pt^{+n}} + Q_{C-CO_x} + Q_{imp} + Q_{Au-AuO_x} \quad \text{(a)}$$

However, we can assume that the current due to the oxidation of gold is nearly constant (i.e., $Q_{Au-AuO_x} = K$) and that the currents generated by processes 1 and 2 are negligible compared to the formation of Pt oxides and to the oxidation of impurities (otherwise, this kind of catalyst will be very unstable). Hence, the expression for Q_T can be simplified:

$$Q_T = Q_{Pt-PtO_x} + Q_{imp} + K \quad \text{(b)}$$

Equation (b) implies that the oxidation of Pt and impurities is responsible for the most important changes in the voltammetric features during the first 10 cycles. Moreover, the first term of Eq. (b) can be estimated by the charge involved in the reduction of Pt oxides, since we can assume that:

$$Q_{Pt-PtO_x} = Q_{PtO_x-Pt} \quad \text{(c)}$$

Then, if Q_{Pt-PtO_x} is subtracted from Eq. (b), the following expression is obtained:

$$Q_T - Q_{Pt-PtO_x} = Q_{imp} + K = \text{NCE} \quad \text{parameter} \quad \text{(d)}$$

The difference between Q_T and Q_{Pt-PtO_x} can be used to monitor the NP cleaning evolution (NCE parameter), because its value depends only on the oxidation of impurities. For an easier comparison, we use the normalized NCE parameter, which is the ratio between the NCE parameter measured at any cycle and the one obtained for cycle 1.

Figure 7b shows the normalized hydrogen oxidation charge (NHOC, which is proportional to the ECSA) and the normalized NCE parameter, in function of the number of voltammetric cycles. The observed changes for NHOC agree with the presence of multiple operating processes causing opposite effects, as already discussed. The increase of ECSA caused by the cleaning of the surface dominates in the first 4 or 5 cycles. Afterward, the curve attains a maximum value (observed between the 4th and 5th cycles in four independent experiments) and then decreases continuously. On the other hand, the NCE parameter shows a continuous decrease. Also, the changes in the NCE parameter are ~100 times more intense than those observed for NHOC. The NCE parameter decreases abruptly in the first cycles (the NPs become cleaner) and agree with the initial increase of ECSA (see Fig. 4b). However, unlike the ECSA, this parameter remains diminishing after the 6th cycle (where the processes

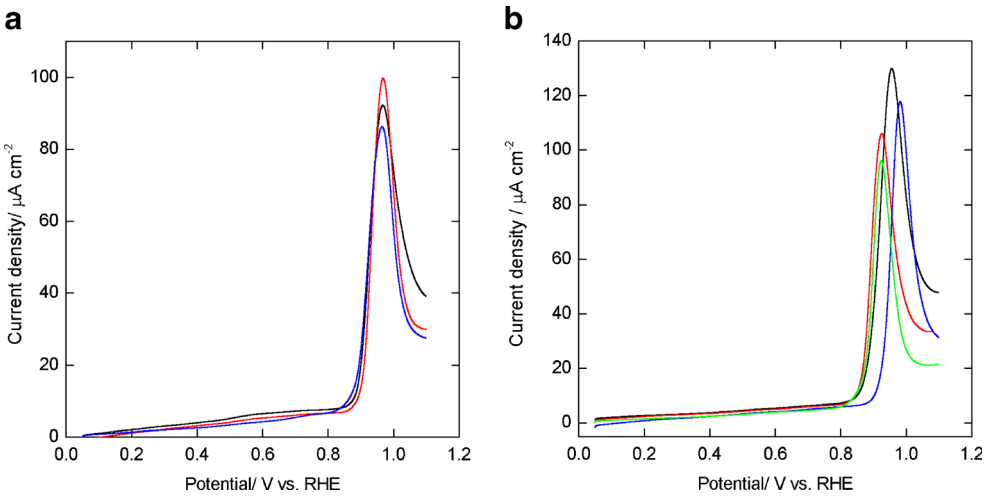

Fig. 9 COEOR performed in 0.5 M H_2SO_4 on clean (**a**) and as-prepared (**b**) PA/Pt=5.0 Pt NPs. v=0.02 V s^{-1}

Table 2 Electrochemical parameters obtained for two series of experiments, with fresh and cycled catalysts

	E_{onset}	SD	SE	E_{peak}	SD	SE	i_{max}	SD	SE
Clean NPs	0.844	0.011	0.006	0.9663	0.0005	0.0003	93	3	1.8
As-prepared NPs	0.835	0.015	0.007	0.947	0.01	0.006	116	6	3

responsible for the decrease of the ECSA dominate the NHOC behavior) and finally tends asymptotically to a constant value.

These experiments allow us to estimate the presence of important amounts of impurities in the as-prepared NPs. Such impurities, in turn, lead to uncertainties in electrochemical experiments, as will be shown in the next section. Thus, we decided to perform the same experiments but using the catalyst of E-TEK® (Pt/C 20 wt%, Fig. 8), because results with this catalyst are spread for all the specific literature. The results of Fig. 8 are quite similar to those obtained with our catalyst, presenting an important presence of impurities that modify the electrocatalytic behavior of the commercial catalyst.

COEOR on Pt NPs. The Relation between Cleaning of NPs and Reproducibility

Figure 9 shows the CO-stripping voltammograms obtained for PA/Pt=5 clean (after 10 cycles, Fig. 9a) and as-prepared NPs (Fig. 9b). Figure 9a presents three independent experiments obtained after 10 cleaning cycles in three different samples, while Fig. 9b shows cyclic voltammograms for four different samples without applying the cleaning process. At a first glance, Fig. 9a, b shows significant differences with regard to reproducibility. In order to quantify those discrepancies we pay attention to some important parameters, namely, (i) the onset potential of CO oxidation (E_{onset}), (ii) the peak potential (E_{peak}), and (iii) the current density at the peak (i_{max}). Table 2 shows the values of these parameters obtained with clean and as-prepared catalyst and the associated errors (standard deviation (SD) and standard error (SE)).

As can be observed in Table 2, all the parameters measured with unclean NPs present more dispersion among them. The fact that the COEOR (on carbon-supported NPs) is severely affected does not only explain the contradictory results found in the literature over the years, but it is feasible to assume that this uncertainty generates significant errors in the determination of current densities whenever the stripping of CO is used for the estimation of ECSA. Besides, the maximum currents obtained for unclean NPs are approximately 20 % higher than those measured after the cleaning process, probably because the oxidation of impurities accounts for the currents of COEOR. This result shows other source of error apart from the uncertainty in the ECSA determination.

Conclusions

- The microwave-assisted synthesis of Pt/C NPs is a facile way to obtain nanoparticles presenting a good dispersion over the support and uniform sizes obtained, provided that the proper amounts of PA were used.
- However, the nanoparticles obtained by this method are partially recovered by impurities left over during the reduction process.
- These impurities impose a lack of control about the state of the surface and generate electrochemical responses poorly reproducible.
- The protocol adopted to clean the surface of the NPs (successive cycles of potential) is able to remove the impurities, but at the same time, the exposed active sites suffer irreversible changes during the cycling process.
- We propose a simple method to follow the NPs cleaning along cycles, which permit to determine the minimum necessary cycles to obtain clean carbon-supported NPs.
- After a few cycles we observe a better reproducibility of the catalytic response (toward the oxidation of CO) with minimum damage of NPs.

Acknowledgments The authors wish to thank to CONICET, CIC, and UNLP. The authors acknowledge financial assistance from CONICET, UNLP, CNPq (Grant # 554591/2010-3), CIC, CAPES, MINCyT and FINEP. P.S. Fernández thanks CONICET (Consejo Nacional de Investigaciones Científicas y Técnicas) for a fellowship. C.A. Martins thanks CNPq for a fellowship (Grant # 140426/2011-6).

References

1. J. Prabhuram, X. Wang, C.L. Hui, I.-M. Hsing, J. Phys. Chem. B **107**, 11057 (2003)
2. W.X. Chen, J.Y. Lee, Z. Liu, Chem. Commun. **21**, 2588 (2002)
3. E.F. Holby, W. Sheng, Y. Shao-Horn, D. Morgan, Energy Environ. Sci. **2**, 865 (2009)
4. S. Rojas, F.J. García-García, S. Jaras, M. Martínez-Huerta, J.L.G. Fierro, M. Boutonnet, Appl. Catal. A Gen. **285**, 24 (2005)
5. B. Fang, N.K. Chaudhari, M.-S. Kim, J.H. Kim, J.-S. Yu, J. Am. Chem. Soc. **131**, 15330 (2009)
6. Y. Wang, J.L. Zhang, X.D. Wang, J.W. Ren, B.J. Zuo, Y.Q. Tang, Top. Catal. **35**, 35 (2005)
7. C. Coutanceau, P. Urchaga, S. Brimaud, S. Baranton, Electrocatalysis **3**, 75 (2012)

8. F.J. Vidal-Iglesias, R.M. Arán-Ais, J. Solla-Gullón, E. Herrero, J.M. Feliu, ACS Catal. **2**, 901 (2012)
9. J. Monzó, M.T.M. Koper, P. Rodriguez, ChemPhysChem **13**, 709 (2012)
10. P.S. Fernández, D.S. Ferreira, C.A. Martins, H.E. Troiani, G.A. Camara, M.E. Martins, Electrochim. Acta **98**, 25 (2013)
11. T.S. Almeida, L.M. Palma, P.H. Leonello, C. Morais, K.B. Kokoh, A.R. De Andrade, J. Power Sources **215**, 53 (2012)
12. W.X. Chen, J.Y. Lee, Z. Liu, Chem. Commun. **8**, 2588 (2002)
13. Z. Liu, L.M. Gan, L. Hong, W. Chen, J.Y. Lee, J. Power Sources **139**, 73 (2005)
14. P.S. Fernández, M.E. Martins, G.A. Camara, Electrochim. Acta **66**, 180 (2012)
15. I.C. McNeill, S.M.T. Sadeghi, Polym. Degrad. Stab. **30**, 213 (1990)
16. O.A. Baturina, S.R. Aubuchon, K.J. Wynne, Chem. Mater. **18**, 1498 (2006)
17. Y. Shao-Horn, W.C. Sheng, S. Chen, P.J. Ferreira, E.F. Holby, D. Morgan, Top. Catal. **46**, 285 (2007)